

## Electrochemical behaviour of vanadium(V)/vanadium(IV) redox couple at graphite electrodes

S. Zhong and M. Skyllas-Kazacos\*

*School of Chemical Engineering and Industrial Chemistry, University of New South Wales, Kensington, NSW 2033 (Australia)*

(Received August 30, 1991)

### Abstract

The electrochemical behaviour of the V(V)/V(IV) couple has been studied at a graphite disc electrode in sulfuric acid using both cyclic and rotating-disc voltammetry. The results from the latter technique have revealed that the cathodic and anodic characteristics of this redox couple are quite different. The diffusion coefficient for V(IV),  $2.14 \times 10^{-6} \text{ cm}^2 \text{ s}^{-1}$ , is independent of the vanadium concentration. For V(IV) oxidation, the electrode kinetic parameters  $i_0$  and  $\alpha$  have values of  $2.47 \times 10^{-4} \text{ A cm}^{-2}$  and 0.71, respectively. The exchange current density,  $i_0$ , for the V(V)/V(IV) reaction has been obtained at both graphite felt and reticulated vitreous carbon electrodes.

### Introduction

As a new and efficient energy storage device, the vanadium redox battery has been widely investigated at the University of New South Wales over the past few years for both theoretical and practical purposes [1-7]. One of the most important aspects of such studies is the electrochemical behaviour of the redox couples at the selected electrode. For the all-vanadium battery, the redox couple for the positive and negative half-cells is V(V)/V(IV) and V(III)/V(II), respectively. During initial screening of redox couples for redox-cell applications, the NASA group [8] used the cyclic voltammetric technique to examine the performance of both vanadium couples. It was reported that the V(V)/V(IV) couple exhibits irreversible behaviour, whereas the reversibility of V(III)/V(II) on a B<sub>4</sub>C electrode was better than that of Cr(III)/Cr(II).

A number of workers [9-12] have investigated the electrochemical behaviour of the V(V)/V(IV) couple at noble-metal electrodes such as platinum and gold. In most cases, it has been found that an oxidation film forms on the electrode surface and subsequently influences the electrochemical reactions. Rychick and Skyllas-Kazacos [3] evaluated the suitability of various electrode materials for the V(V)/V(IV) reactions. The findings indicated that the redox reactions are irreversible on gold and glassy-carbon electrodes. On lead and titanium electrodes, however, passivating phenomena were observed over the potential range of interest. Although platinized titanium and DSA (dimensionally stable anode) electrodes exhibited no such problem and gave better reversibility, the high cost of these materials would be prohibitive for large-scale applications of the vanadium battery.

\*Author to whom correspondence should be addressed.

Sum *et al.* [5] also studied the kinetics of the V(V)/V(IV) couple on glassy-carbon and gold electrodes with cyclic voltammetry and rotating-disc voltammetry. It was concluded that the system is electrochemically irreversible with a value of the standard heterogeneous rate constant,  $k^0 = 7.5 \times 10^{-4} \text{ cm s}^{-1}$  and a diffusion coefficient of  $1.4 \times 10^{-6} \text{ cm}^2 \text{ s}^{-1}$  for V(V). It was also found that the electrochemical behaviour of the V(V)/V(IV) couple on a glassy-carbon electrode is affected greatly by the procedure used for surface preparation.

As pointed out by Miller and Zittle [13], at a pyrolytic graphite electrode, cathodic voltammograms are reproducible and there is no evidence that the surface of the electrode is oxidized by contact with V(V). This implies that this material is suitable for examining the electrochemical behaviour of the V(V)/V(IV) redox couple. On the other hand, electrodes based on graphite felt are employed in both the positive and negative sides of the vanadium redox battery and high efficiencies have been achieved with this material [7]. It is thus desirable to establish the electrode kinetics of the V(V)/V(IV) redox reactions at graphite electrodes. The kinetic studies have been performed using both cyclic voltammetry and rotating-disc voltammetry. The diffusion coefficient for V(IV) and the electrode kinetic parameters have also been calculated. Finally, the equilibrium exchange-current density values for the V(V)/V(IV) couple have been determined for graphite felt and reticulated vitreous carbon electrodes.

## Experimental

The electrochemical behaviour of the V(V)/V(IV) couple was studied at a graphite electrode (area =  $0.096 \text{ cm}^2$ , CMG, Carbon Brush MFG Pty Ltd, Rosebery, Australia) using rotating-disc voltammetry. Two types of electrolyte were employed: (i)  $\text{VOSO}_4$  (Merck, BDH Chemical Australia Pty Ltd) of various concentrations in 3 M  $\text{H}_2\text{SO}_4$ ; (ii) 50:50 mixture of V(IV) and V(V), this corresponds to a 50% state-of-charge (SOC) positive vanadium redox cell solution. The latter was prepared by mixing equal volumes of V(IV) solution (0% SOC) with V(V) solution (100% SOC, obtained by fully charging the V(IV) solution to V(V) in the positive half-cell of a vanadium redox cell).

The graphite electrode was polished with 600 (= P1200)-grit silicon carbide polishing paper, followed successively by 800-grit Flexboc polishing paper and by  $0.3 \mu\text{m}$  alumina (Buehler Ltd, Lake Bluff, IL, USA) on polishing cloth (LECO Corporation, Michigan, USA). Each electrode was rinsed thoroughly with distilled water and then subjected to ultrasonification for 15 min using an Ultrasonic cleaner (LECO Corporation, Michigan, USA). The graphite felt and reticulated vitreous carbon (RVC) electrodes were produced by heat-pressing a piece of graphite felt and RVC on one side of a conducting plastic sheet [14]. The latter had a copper-foil backing. The geometric surface area of the electrodes was  $1 \text{ cm}^2$ .

The cathodic and anodic linear-sweep voltammograms and the cyclic voltammograms were obtained with a Pine RD3 potentiostat (Pine Instrument Co., Grove City, PA, USA) and a model D Riken Denshi X-Y recorder. The electrode rotating speed was controlled by a MSR speed controller (Pine Instrument Co.) combined with a Type D824-16 Bi-Mode Torque Unit (Servo-Tek Production Co., Hawthorn, NJ, USA). All potentials were measured against a  $\text{Hg}/\text{Hg}_2\text{SO}_4$  reference electrode and are reported with respect to this electrode. A pure platinum wire was used as the counter electrode. Cathodic or anodic linear-sweep voltammograms were always started from the static potential. The cathodic voltammogram was obtained prior to the anodic scan. With cyclic voltammetric studies, however, the initial scan direction was always positive.

## Results and discussion

### Reproducibility of electrode surface preparation

Sum *et al.* [5] previously reported that the preparation procedure for the electrode surface has a critical effect on the electrode kinetics of the vanadium redox couples at a glassy-carbon electrode. The first objective, therefore, was to examine the reproducibility of the surface preparation procedure on the behaviour of the graphite electrode. Figure 1(a) shows three anodic voltammograms that were obtained after successively repolishing the graphite electrode surface using the procedure described above. The curves are for the first sweep after polishing and demonstrate that the reproducibility obtained on the graphite electrode surface is much better than that achieved for a glassy-carbon surface [4, 5]. Figure 1(b) illustrates the cyclic stability of the graphite electrode during the initial 10 cycles over the potential range 0 to +1.10 V. Apart from the first cycle, only a slight variation can be observed among the remaining voltammograms. This confirms that the graphite electrode is a suitable working electrode for studying the electrochemical behaviour of the V(V)/V(IV) redox couple.

### Cyclic voltammetry

A series of cyclic voltammograms corresponding to the V(V)/V(IV) redox couple at the graphite electrode at various sweep rates in 0.1 M 50% SOC positive vanadium redox cell solution is presented in Fig. 2(a) for the potential range of  $-0.504$  to  $+0.90$  V. Four peaks (marked as A, B, C and D) are observed in each cyclic voltammogram. This suggests that besides the expected V(V)/V(IV) redox reactions, there are other electrochemical processes taking place during the potential scanning. From comparison with the cyclic voltammograms obtained at the same graphite electrode in 3 M  $\text{H}_2\text{SO}_4$  and under the same experimental conditions (Fig. 2(b)), it can be seen that the given several peaks, associated with the carbon-oxygen surface reaction, interfere with the vanadium reactions. When the potential is limited to between 0 and 0.9 V, however, this interference from carbon-oxygen surface reactions is minimized, see Fig. 3.

### Rotating-disc voltammetry

In order to obtain more information on the electrode kinetics of the V(V)/V(IV) couple on graphite electrodes, cathodic and anodic voltammetric experiments were

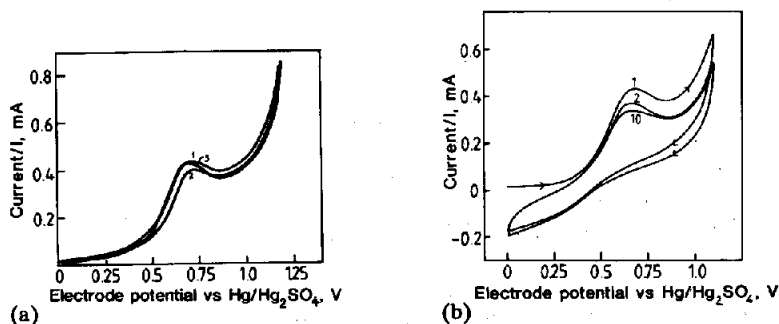


Fig. 1. Cyclic voltammograms for graphite electrode in 0.1 M  $\text{VOSO}_4/3$  M  $\text{H}_2\text{SO}_4$  solution, sweep rate:  $10 \text{ mV s}^{-1}$ ; (a) anodic scans for testing reproducibility of surface preparation; (b) cyclic scans for testing the cyclic stability, 1st to 10th cycle.

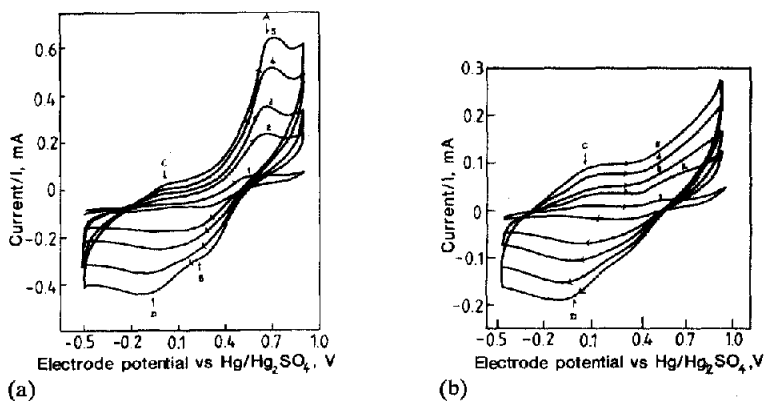


Fig. 2. Cyclic voltammograms for graphite electrode in: (a) 0.05 M V(V)+0.05 M V(IV) in 3 M H<sub>2</sub>SO<sub>4</sub>; (b) 3 M H<sub>2</sub>SO<sub>4</sub>. Scan rates: 1, 10, 20, 40, 60 mV s<sup>-1</sup> for curves 1 to 5, respectively.

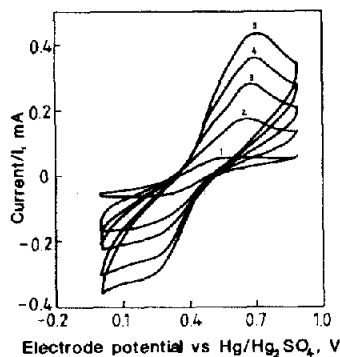


Fig. 3. Cyclic voltammograms for graphite electrode over the potential range 0 to 0.9 V. Other conditions are the same as those given for Fig. 2(a).

also performed with a rotating-disc electrode in the same solution as that used to gather the data given in Figs. 2(a) and 3. A potential sweep rate of 1 mV s<sup>-1</sup> was employed and the electrode rotation speed was varied between 60 and 2400 rpm. The current (*i*) versus overpotential ( $\eta$ ) curves, recorded in Fig. 4(a) and (b), show that, at each rotation speed, cathodic and anodic limiting currents are obtained. The magnitude of these currents increases with electrode rotation speed and this indicates that the electrode processes become mass-transfer controlled [15].

The *i*- $\eta$  curves also reveal that the cathodic and anodic electrode processes are quite different. In the anodic voltammograms, for example, there is only one wave (corresponding to V(IV) being oxidized to V(V)), while in the cathodic voltammograms at least two waves have to be considered. This indicates that besides the main V(V) species, other species such as V(V)-SO<sub>4</sub><sup>2-</sup> complexes [16] or carbon-oxygen surface complexes [17] (see Fig. 2(b)) are reduced within this potential range.

Figure 4(b) shows the cathodic and anodic voltammograms obtained at electrode rotation speeds between 1200 and 2400 rpm. Unlike the curves obtained at lower rotation speeds, the *i*- $\eta$  curves are very close, particularly in the anodic branch. The

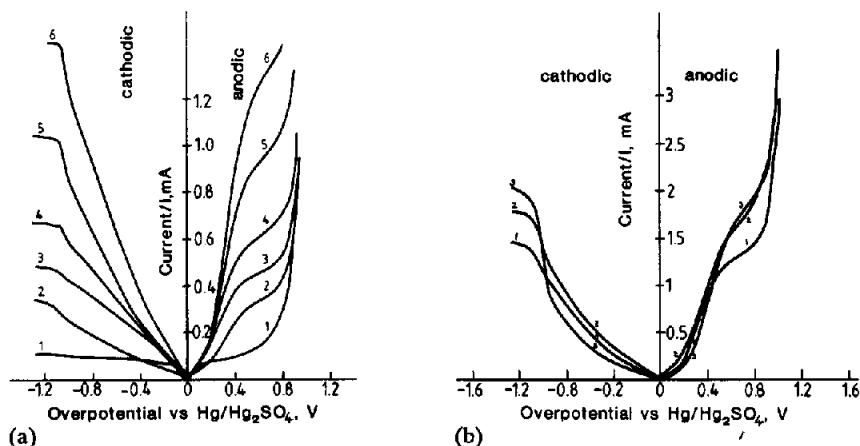


Fig. 4. Cathodic and anodic voltammograms for a rotating-disc graphite electrode in the electrolyte of Fig. 2(a). Scan rate:  $1 \text{ mV s}^{-1}$ ; (a) rotation speeds: 0, 60, 120, 240, 600, 1200 rpm for curves 1 to 6, respectively; (b) rotation speeds: 1200, 1800, 2400 rpm for curves 1 to 3, respectively.

TABLE 1

Limiting currents obtained at various angular speeds

$\omega^{1/2}$ ( $\text{S}^{-1/2}$ )	$i_{L,c}$ ( $\text{A cm}^{-2}$ )	$i_{L,a}$ ( $\text{A cm}^{-2}$ )
2.51	$3.44 \times 10^{-3}$	$3.44 \times 10^{-3}$
3.54	$5.00 \times 10^{-3}$	$4.69 \times 10^{-3}$
5.01	$6.88 \times 10^{-3}$	$6.46 \times 10^{-3}$
7.93	$10.83 \times 10^{-3}$	$10.21 \times 10^{-3}$
11.21	$15.10 \times 10^{-3}$	$14.06 \times 10^{-3}$
13.73	$18.23 \times 10^{-3}$	$17.19 \times 10^{-3}$
15.85	$20.83 \times 10^{-3}$	$18.23 \times 10^{-3}$

anodic curve obtained at 2400 rpm is almost the same as that at 1800 rpm. This indicates that, at sufficiently high rotation speeds, the electrode process is no longer diffusion controlled but becomes influenced by kinetic features.

#### Diffusion coefficient

The diffusion coefficient of the V(IV) reactive species was determined from the Levich equation:

$$i_L = 0.62408nFD^{2/3}\nu^{-1/6}\omega^{1/2}C_b \quad (1)$$

where:  $i_L$  is limiting current density;  $n$  is the number of electrons participating in the reaction;  $D$  is the diffusivity of reactive species;  $\nu$  is the viscosity of electrolyte;  $\omega$  is the angular speed of rotation;  $C_b$  is the concentration of reactive species in the bulk electrolyte;  $F$  is the Faraday constant.

A summary of limiting currents and corresponding angular speed obtained directly from Fig. 4(a) and (b) is given in Table 1. To avoid introducing error caused by the interference of the other reactants discussed above, only anodic curves were analysed.

A linear relationship is found between the square root of the angular speed and the anodic limiting current density (Fig. 5). This demonstrates that up to a electrode rotation speed of 1800 rpm, the V(IV) oxidation reaction obeys the Levich equation. From the slope of the linear plots, the diffusion coefficient for V(IV) was calculated as  $2.00 \times 10^{-6} \text{ cm}^2 \text{ s}^{-1}$ .

Rotating-disc voltammograms were also obtained for a range of vanadium concentrations. The latter was varied from 0.01 to 0.5 M, and electrode rotation speeds of 120, 360, 720 and 1080 rpm were employed. Figure 6 shows typical anodic voltammograms obtained in 0.5 M  $\text{VOSO}_4$  solution. The anodic limiting current density ( $i_{L,a}$ ) was plotted versus the square root of angular speed at each concentration; the results are given in Fig. 7(a). The anodic limiting current density versus vanadium concentration was also plotted to yield Fig. 7(b). The linear relationships obtained in both Fig. 7(a) and (b) illustrate that the V(IV) oxidation reaction at these concentrations obeys the Levich equation. Plots of limiting current density divided by vanadium concentration as a function of the square root of the angular speed are presented in Fig. 8. The diffusion coefficients were determined from the slopes of the resulting straight lines and are listed in Table 2. From the values, it can be concluded that,

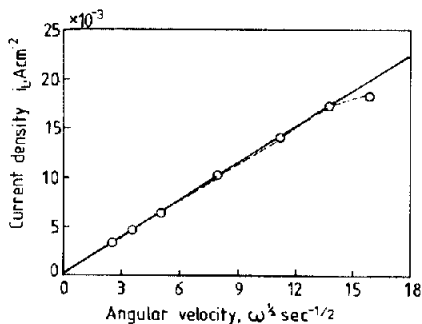


Fig. 5. Plot of limiting current density ( $i_L$ ) vs square root of angular speed for anodic voltammograms of Fig. 4.

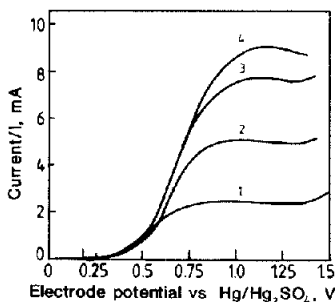


Fig. 6. Anodic rotating-disc voltammograms for a graphite electrode in 0.5 M V(IV)/3 M  $\text{H}_2\text{SO}_4$  solution; rotation speeds: 120, 360, 720, 1080 rpm for curves 1 to 4, respectively.

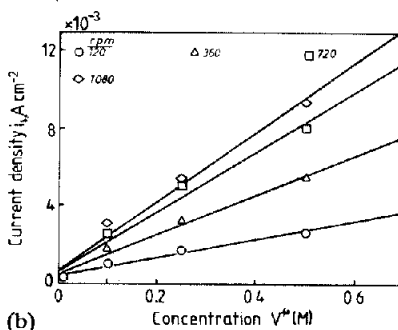
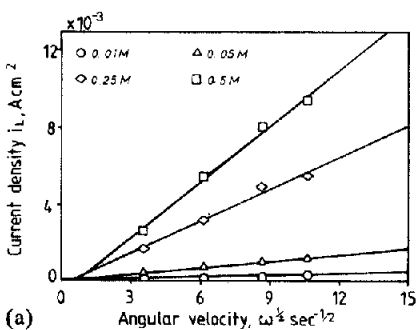


Fig. 7. (a) Plot of anodic limiting current density vs. square root of angular speed at various vanadium concentrations; (b) plot of anodic limiting current density vs. vanadium concentration at various electrode rotation speeds.

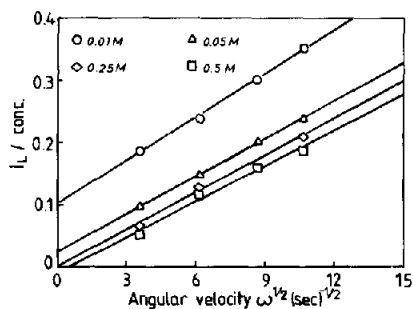


Fig. 8. Plot of  $i_{L,a}$ /vanadium concentration vs. square root of angular speed for anodic voltammograms of Fig. 6 at various vanadium concentrations.

TABLE 2

Diffusivity of V(IV) species

V(IV) concentration (mol cm <sup>-3</sup> )	Diffusion coefficient (cm <sup>2</sup> s <sup>-1</sup> )
$0.01 \times 10^{-3}$	$2.46 \times 10^{-6}$
$0.05 \times 10^{-3}$	$2.00 \times 10^{-6}$
$0.25 \times 10^{-3}$	$2.25 \times 10^{-6}$
$0.5 \times 10^{-3}$	$1.86 \times 10^{-6}$

over the given concentration range, the diffusion coefficient of the V(IV) species is essentially constant with an average value of  $2.14 \times 10^{-6}$  cm<sup>2</sup> s<sup>-1</sup>.

#### Kinetic parameters

For an electrode reaction that is activation controlled, the exchange current density,  $i_0$ , and transfer coefficient,  $\alpha$ , can be determined from the well-known Tafel equation. For an electrode process subject to mass transport, the following equation applies [15]:

$$\eta = - \frac{RT}{(1-\alpha)nF} \ln \frac{i_0}{i_{L,a}} - \frac{RT}{(1-\alpha)nF} \ln \frac{i_{L,a}-i}{i} \quad (2)$$

where:  $\eta$  is anodic overpotential;  $R$  is the normal gas constant;  $T$  is the temperature;  $i$  is the measured anodic current density. (All other parameters as defined above). Equation (2) indicates that the anodic overpotential should be linearly related to  $\ln(i_{L,a}-i)/i$  and that  $i_0$  and  $\alpha$  can be determined from the intercept and the slope of the resulting straight line.

For an anodic current within the range  $0.1 i_{L,a} < i < 0.9 i_{L,a}$ , which is normally considered to be the combined mass-transport and surface-activation region, from the anodic voltammograms shown in Fig. 4(a) and (b), the anodic overpotential was plotted against  $\log(i_{L,a}-i)/i$  at each rotation speed. The results are presented in Fig. 9. The  $i_0$  and  $\alpha$  values were obtained from the intercepts and the slopes of the straight lines, and are summarized in Table 3. The average values for  $i_0$  and  $\alpha$  were  $2.47 \times 10^{-4}$  A cm<sup>-2</sup> and 0.71, respectively. The low value of the exchange current density indicates that the kinetics of the V(V)/V(IV) couple at the graphite electrode are slow. The

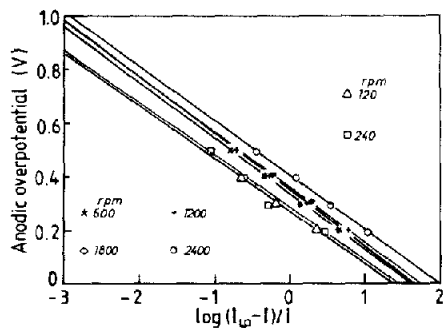


Fig. 9. Plot of anodic overpotential vs.  $\log(i_{L,a}-i)/i$  from voltammograms of Fig. 4.

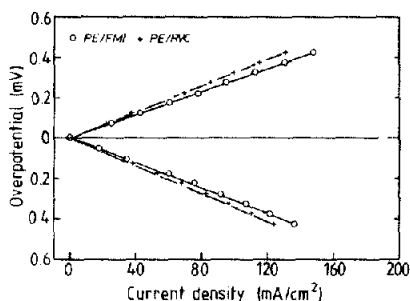


Fig. 10. Cathodic and anodic polarization curves for graphite felt (PE/FMI) and reticulated vitreous carbon (PE/RVC) electrodes in 1.0 M V(V)+1.0 M V(IV) in 3 M H<sub>2</sub>SO<sub>4</sub>.

TABLE 3

The kinetic parameters of V(V)/V(IV) couple

Electrode rotation speed (rpm)	Transfer coefficient ( $\alpha$ )	Exchange current density ( $i_0$ , A cm <sup>-2</sup> )
60	0.73	$1.18 \times 10^{-4}$
120	0.70	$2.09 \times 10^{-4}$
240	0.70	$2.67 \times 10^{-4}$
600	0.72	$2.71 \times 10^{-4}$
1200	0.71	$2.84 \times 10^{-4}$
1800	0.72	$4.18 \times 10^{-4}$
2400	0.71	$1.61 \times 10^{-4}$

high value for  $\alpha$  demonstrates the asymmetry in the activation energy peak for this electrochemical system. The low value of  $i_0$  could also be associated with a low effective surface area for the electrode reactions at the graphite electrode. In the practical cells and batteries, these problems are overcome by using a graphite felt of high surface area (600 g m<sup>-2</sup>) in place of the flat graphite plate.

Figure 10 shows the cathodic and anodic voltammograms obtained at graphite felt and reticulated vitreous carbon electrodes in 50% SOC vanadium solution under static electrolyte condition. The curves were recorded manually. A linear relationship is observed between the electrode overpotential and the current density on both electrodes. Plotting the overpotential versus current density in the range of  $\pm 50$  mV and using the Linear Polarization equation [15], the  $i_0$  value was determined as  $0.92 \times 10^{-2}$  A cm<sup>-2</sup> for graphite felt and  $0.80 \times 10^{-2}$  A cm<sup>-2</sup> for RVC. The values are significantly higher than those obtained at the graphite disc electrode and are due to the higher surface area of these electrodes. In spite of the high surface area, however, the kinetics of the V(V)/V(IV) reactions are limited by the number of active sites on the carbon and graphite surfaces. Further improvements in the effective surface area have been achieved by the application of various surface-activation treatment methods. These procedures have been successfully used to increase the number of



active sites for the V(V)/V(IV) redox couple reaction on graphite felt electrodes with the result that energy efficiencies of up to 90% have been achieved in the vanadium redox cell [18].

## Conclusions

The kinetics of the V(V)/V(IV) redox couple reaction have been found to be electrochemically irreversible at flat graphite electrodes. Rotating-disc voltammetry studies reveal that the diffusivity of V(IV) species is independent of vanadium concentration and that the value of the diffusion coefficient is  $2.14 \times 10^{-6} \text{ cm}^2 \text{ s}^{-1}$ . Although the exchange current density at a flat graphite electrode is low, it is increased by two orders of magnitude at the graphite felt electrode. The latter material is therefore more suitable for use in the vanadium redox cell.

## Acknowledgements

This project has been funded by a grant from the Australian Research Council.

## References

- 1 M. Skyllas-Kazacos and R. Robins, *US Patent App. 849 094* (1986).
- 2 M. Skyllas-Kazacos and F. Grossmith, *J. Electrochem. Soc.*, **134** (1987) 2950.
- 3 M. Rychcik and M. Skyllas-Kazacos, *J. Power Sources*, **19** (1987) 45.
- 4 E. Sum and M. Skyllas-Kazacos, *J. Power Sources*, **15** (1985) 179.
- 5 E. Sum, M. Rychcik and M. Skyllas-Kazacos, *J. Power Sources*, **16** (1985) 85.
- 6 M. Rychcik and M. Skyllas-Kazacos, *J. Power Sources*, **22** (1988) 59.
- 7 M. Kazacos and M. Skyllas-Kazacos, *J. Electrochem. Soc.*, **136** (1989) 2759.
- 8 US Dept. of Energy, *NASA TM-79067*, (1979) 49.
- 9 F. C. Anson and D. M. King, *Anal. Chem.*, **34** (1962) 362.
- 10 D. G. Davis, *Talanta*, **3** (1965) 335.
- 11 F. Z. Dzhabarov and S. V. Gorbachev, *Russ. J. Phys. Chem.*, **38** (1964) 911.
- 12 T. D. Cebelka, D. S. Austin and D. C. Johnson, *J. Electrochem. Soc.*, **131** (1984) 1595.
- 13 F. J. Miller and H. E. Zittle, *J. Electroanal. Chem. Interfacial Electrochem.*, **7** (1964) 116.
- 14 S. Zhong, M. Kazacos, R. P. Burford and M. Skyllas-Kazacos, *J. Power Sources*, **36** (1992) 29.
- 15 A. J. Bard and L. R. Faulkner, *Electrochemical Methods – Fundamentals and Applications*, Wiley-Interscience, New York, 1980, p. 102 and p. 110.
- 16 M. Kazacos, Electrolyte optimisation and electrode material evaluation for the vanadium redox battery, *Ph.D. Thesis*, Univ. of NSW, Australia, 1989, pp. 135–136.
- 17 T. C. Golden, R. G. Jenkins, Y. Otake and A. W. Scaroni, *Proc. Workshop on Electrochemistry of Carbon*, The Electrochemical Society, Pennington, NJ, Vol. 84–5, 1984, p. 61.
- 18 B. Sun, Studies in electrode activation for vanadium redox flow battery application, *Ph.D. Thesis*, Univ. of NSW, Australia, 1991.